A COMPREHENSIVE STUDY OF TITAN'S MAGNETIC PILE-UP REGION DURING THE CASSINI ERA

A Dissertation
Presented to
The Academic Faculty

By

Chen Chen

In Partial Fulfillment
of the Requirements for the Degree
Master of Science in the
School of Earth and Atmospheric Sciences

Georgia Institute of Technology

May 2020

A COMPREHENSIVE STUDY OF TITAN'S MAGNETIC PILE-UP REGION DURING THE CASSINI ERA

Approved by:

Dr. Sven Simon, Advisor
School of Earth and Atmospheric Sciences
Georgia Institute of Technology

Dr. Zhigang Peng
School of Earth and Atmospheric Sciences
Georgia Institute of Technology

Dr. James Wray
School of Earth and Atmospheric Sciences
Georgia Institute of Technology

Date Approved: April 15, 2020

ACKNOWLEDGEMENTS

I would like to first thank my advisor Dr. Sven Simon for his guidance, patience and quick responses to my questions. I would also like to thank my thesis committee members, Dr. Zhigang Peng and Dr. James Wray, for reading this thesis and providing meaningful suggestions. I would like to acknowledge Dr. Greg Huey, Dr. Martial Taillefert, Dr. Yuanzhi Tang, Dr. Yuhang Wang and Dr. Chris Reinhard for their help, suggestions, and encouragement.

Many thanks to graduate students for the helpful advice on both academic and personal life – Hannes, Clara, Lindsay, Chenyu, Qiushi, Zijian, Pengxiao, Qiyang, Mingyu, Kezhen, Yi, Kezhou, Pan and Simin.

My work cannot be done with the help of many people who build the Planetary Data System and make Cassini data available.

Last but not least, I would like to thank my friends and family for always being there whenever I need help or encouragement.

TABLE OF CONTENTS

LIST OF TABLES

LIST OF FIGURES

SUMMARY

Because Saturn's largest moon Titan is devoid of an intrinsic magnetic field, draping of the giant planet's magnetospheric field around Titan's ionosphere generates a pile-up region at the moon's ramside (the hemisphere of Titan facing the incident plasma flow of Saturn's magnetosphere). A single close flyby of previous Voyager 1 mission presented a quiet magnetic field and plasma conditions around Titan with no significant fluctuations. But data from the recent Cassini mission provided a comprehensive picture of Titan's plasma environment. In this thesis, Cassini magnetic field data from all 126 Titan flybys are systematically analyzed to characterize the extensions and magnitudes of the pile-up region. Along each flyby trajectory, we determine the segments where Cassini crossed the piled-up magnetic field, and generate altitude profiles of the pile-up strength. Furthermore, we investigate the dependency of the extension and strength of the pile-up region on various parameters, such as the Saturn local time and the magnetospheric environment to which Titan is exposed. In this way, a comprehensive picture of Titan's ramside magnetic barrier during the Cassini era is generated. We suggest that Titan's magnetic pile-up region is qualitatively stable under different Saturn local times and magnetospheric environments. However, the observational bias exists due to the limited number of flybys, future works are needed for further investigations. A paper on this work will be published in the near future.

CHAPTER 1

INTRODUCTION

Titan, the largest moon in the Saturnian system, orbits Saturn at a distance of 20.3 R_S (R_S=60268 km) and has a radius of R_T=2575 km. Before the Cassini mission, our knowledge about the plasma interaction between Titan and its magnetospheric environment was solely based on data from a single close flyby of Voyager 1 in November 1980, revealing an ambient magnetospheric field nearly perpendicular to Titan's orbital plane, and no significant fluctuations in the magnetic field and plasma conditions outside of Titan's interaction region [1]. However, between 2004 and 2017, the Cassini spacecraft completed 126 close flybys of Titan, which have provided us with a comprehensive picture of the moon's plasma environment. Because of the absence of an intrinsic magnetic field [2, 3], Titan's exosphere and ionosphere are directly exposed to Saturn's magnetospheric plasma flow. At the ramside, the plasma flow is diverted due to mass loading from Titan's ionosphere, and thus Saturn's magnetospheric field drapes around the highly conducting ionosphere of Titan, generating a pile-up region [2, 4] as shown in Figure 1.1. This region is characterized by an enhancement of the magnetic field, and the draping of the magnetic field extends to the moon's wakeside as the magnetotail lobes [5]. Numerical simulations [6, 7] suggest that this magnetic barrier possesses a pronounced asymmetry between Titan's Saturn-facing and Saturn-averted hemispheres, which is caused by the large gyroradii of pick-up ions. This leads to an asymmetry of the pile-up region along the direction of the convective electric field $\vec{E_0} = -\vec{u_0} \times \vec{B_0}$, where $\vec{u}_0$ is the bulk velocity of the corotating magnetospheric plasma and $\vec{B_0}$ denotes the magnetospheric background field. Previous studies (e.g., [8]) also revealed that an asymmetry of the pile-up between Titan's northern and southern hemispheres is developed by a non-vanishing component of the magnetospheric background field along the corotational flow direction.

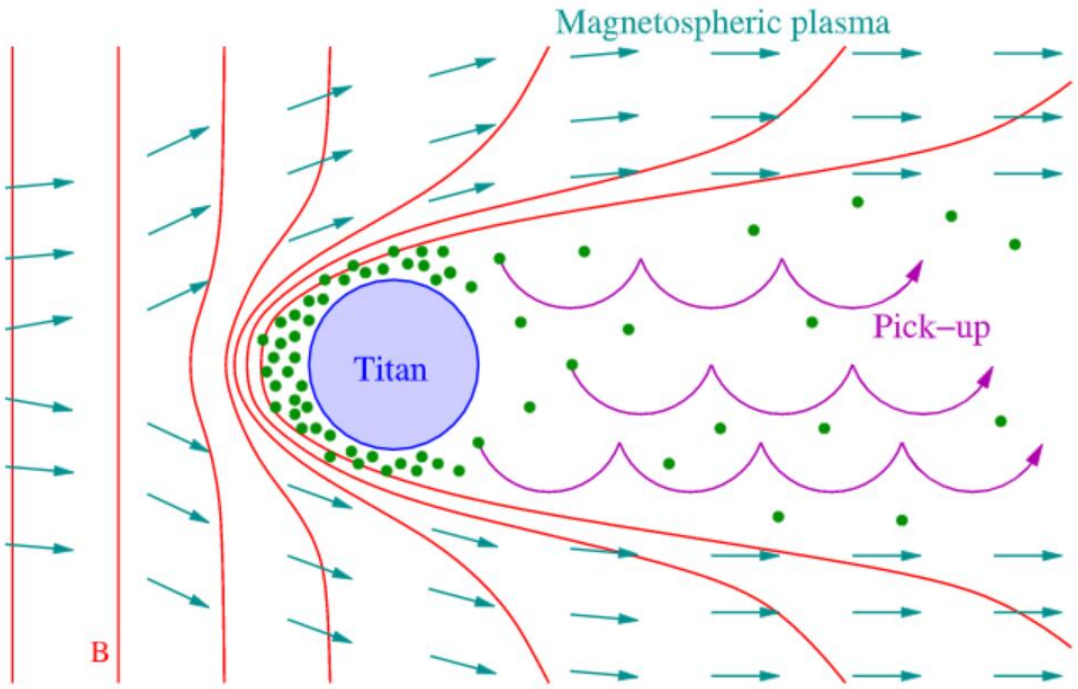

Figure 1.1: A schematic illustration of the plasma and magnetic field perturbations near Titan. (Adopted from [9])

The relation between the structure of Titan's induced magnetosphere and the orientation of the illuminated side of its ionosphere with respect to the incident plasma flow has been studied by Ledvina et al. (2012) [10]. Using a hybrid code and considering Titan under 3 different Saturn local times (06:00, 12:00 and 18:00), they found that the ion loss rates and the electromagnetic field have only a weak quantitative dependence on the solar illumination angle. This result is consistent with the study of Simon et al. (2007) [11] who modeled Cassini magnetic field data from the T9 flyby. These authors showed that the magnetic field topology near Titan is nearly independent of the ionospheric ion production rate: a decrease of the production rate by a factor of ≈ 3 was found to generate only a slight change in the magnetic field along Cassini's trajectory. These modeling studies suggest that the structure of the draped magnetic field near Titan has little dependence on both, the angle and intensity of solar illumination. However, the density of Titan's ionosphere depends on the solar illumination angle and solar cycle. It increases during the solar maximum due

to increased EUV fluxes. Additionally, the distance from Saturn to the Sun varies by up to 1 AU over a Saturnian year, leading to a 25 $\%$ change of EUV flux. Therefore, the orbital phase of Saturn is critical for the structure of Titan's ionosphere [12].

Titan's induced magnetosphere is also affected by the presence of Saturn's dynamic magnetodisk. This magnetodisk consists of the highly stretched magnetic field, surrounding the magnetically confined plasma in the equatorial plane of Saturn [13]. Arridge et al. (2008) [14] showed that the shape of Saturn's magnetodisk is highly responsive to the upstream solar wind pressure. Under the high pressure where the subsolar magnetopause standoff distance is below 20 R_S, the dayside magnetodisk cannot be formed and the field near noon local time shows a quasi-dipolar configuration. This is consistent with the results of Simon et al. (2010) [15] who characterized Titan's magnetospheric environment during TA-T62 on a flyby-to-flyby basis and found that in Saturn's dayside magnetosphere, Titan was frequently embedded in strongly distorted current sheet fields due to the suppression of the magnetodisk by the proximity to Saturn's magnetopause.

Furthermore, the configuration of Saturn's magnetosphere near Titan's orbit exhibits large-scale seasonal changes since the magnetic dipole moment of Saturn is almost aligned with its rotation axis and is *not* perpendicular to that of the incident solar wind (except for the equinoxes). This seasonal change causes Saturn's current sheet to be deformed into a bowl open toward the north/south in southern/northern summer. Therefore, the orbit of Titan is on average located below the current sheet and embedded in the southern magnetodisk lobe during southern summer, while Titan's orbit is on average located above the current sheet and exposed to the northern magnetodisk lobe during northern summer [16, 13].

Considering all 126 Titan flybys, a comprehensive picture for the seasonal variations of Titan's ambient magnetospheric field was presented by Kabanovic et al. (2017) [17]. These authors demonstrated that in the dayside magnetosphere, the magnetic field near Titan shows little seasonal variability. However, in the nightside magnetosphere, a slow

but steady variation in the magnetospheric background field at Titan's orbit was discerned throughout the Cassini era, showing a change from southern lobe-type to northern lobe-type. This shift is consistent with the seasonal change in the curvature of Saturn's magnetodisk current sheet. As found by, e.g., [18], [19] and [20], when embedded in Saturn's magnetodisk lobes, Titan is exposed to a dilute, low plasma beta ($\beta \ll 1$), consisting mainly of light H^+ and H_2^+ ions. However, when Titan is embedded in Saturn's magnetodisk current sheet the incident plasma possesses a higher beta value ($\beta \approx 1$ or $\beta \gg 1$) and consists mainly of heavy ions (mass $\approx 17\mathrm{amu}$).

In addition, the magnetospheric field near Titan oscillates with a period close to Saturn's rotation period of about 10.7 h [21]. As revealed by Simon et al. (2010) [15], Titan's immediate magnetic environment is distorted by the oscillating current sheet on time scales between only a few minutes and about 5 h (with the latter value corresponding to half a period of Saturn's rotation). In magnetic field data, these magnetospheric oscillations can be seen as a continuous change from the northern magnetodisk lobe (where the field points away from Saturn) to the southern magnetodisk lobe (where the field points toward Saturn), see [13].

Based on the magnetic field data from Cassini flybys TA-T85, the response of Titan's induced magnetotail to these varying background field conditions was analyzed by Simon et al. (2013) [22]. They found that when Titan is embedded in the southern or northern lobe of Saturn's magnetodisk, the moon's induced magnetosphere can be described well by the idealized steady-state draping picture, which means the signs of the observed B_X perturbations (where the X direction is aligned with the corotational flow) agree with the notion of draping the average magnetospheric field around Titan's conducting ionosphere [8]. Even when Titan is exposed to the perturbed current sheet fields, the picture of draping the average background field around Titan's ionosphere is still applicable to explain the magnetic field data from more than 60% of Titan flybys that occurred in that magnetospheric regime. However, during flybys that found Titan exposed to intense north-south

oscillations of Saturn's magnetodisk current sheet, the characteristic draping pattern is obscured by the ambient magnetospheric perturbations.

However, while Simon et al. (2013) [22] investigated the structure of Titan's magnetotail in various magnetospheric upstream regimes, it is still unclear how Titan's pile-up region responds to the ambient magnetospheric field regime. Another open question is whether observations reveal a dependency of the pile-up on the moon's orbital position. Therefore, a comprehensive picture of Titan's pile-up region will be developed in this study, using all available Cassini magnetic field data. In section 2, we present our selection criteria for the magnetic field datasets as well as our analysis method. Subsequently, our results will be shown in section 3, where we will illustrate the spatial structure of the pile-up region. We will investigate possible dependencies of the pile-up region on local time and Titan's ambient magnetic environment. A brief summary of our study is presented in section 4.

CHAPTER 2

DATA SELECTION AND ANALYSIS METHOD

In this section, the criteria for identification of Titan's ramside pile-up region in magnetic field data are introduced. Subsequently, we demonstrate the application of these criteria to two selected flybys: T88 and T108. We also show one example that is *excluded* by our criteria: T89. The trajectories of these encounters are shown in Figure 2.1 (a), whereas the corresponding magnetic field data sets are displayed in Figures 2.1 (b), (c), and (d), respectively.

All 126 Titan flybys during the Cassini era are initially considered in this study. We apply the Cartesian Titan Interaction System (TIIS) with Titan's center at the origin and the X, Y, and Z axes pointing along the corotation direction, from Titan toward Saturn, and northward [4]. The MAG data that Cassini obtained within the cube $-10R_T < X, Y, Z < 10R_T$ during each flyby are initially considered in our study.

Besides the ramside pile-up region, other structures of Titan's induced magnetosphere, such as the downstream magnetic lobes, and ambient magnetospheric field fluctuations could also generate signatures of enhanced $|\vec{B}|$, which are unrelated to the pile-up at Titan's ramside. To make sure that the field enhancements we consider are actually associated with Titan's ramside pile-up region, several selection criteria are introduced:

(1) The trajectory of the Cassini spacecraft should pass through the ramside hemisphere of Titan ($X < 0$) within 4 R_T of the center of Titan, which will cover the range of distances where the pile-up region is typically located (e.g., [7]). As suggested by various models, the pile-up region not only wraps around Titan at the ramside, but is also highly asymmetric: it possesses a much larger extension into the direction of the convective electric field $\vec{E_0} = -\vec{u_0} \times \vec{B_0}$ which points away from Saturn. The cycloidal arcs of the nitrogen pick-up ions possess an extension about 5.4 R_T in the direction of $\vec{E_0}$ [23]. Furthermore,

the draping pattern and associated pile-up possess asymmetries between the northern and southern hemispheres or between the Saturn-facing and Saturn-averted hemispheres when the ambient field has a non-zero B_{0X} or B_{0Y} component.

(2) A distinct enhancement with the maximum magnetic field magnitude way above the background level, should be discernible in MAG data during the crossing of Titan's ramside hemisphere. To be more precise, since the pile-up may not only be located in the ramside hemisphere but also wrap around Titan and slightly penetrate into the $X > 0$ hemisphere (e.g., [6] and [7]), the data point with the maximum magnitude should be located in the region of $X < 0.5\ R_T$. In some cases, Cassini has initially passed through the pile-up region, and then came close to the ionopause (the altitude of which is around 1400 km to 2150 km [24]), and subsequently re-enter the pile-up region during the outbound leg of the flyby. Correspondingly, the value of $|\vec{B}|$ will enhance at first, then decrease, and then increase again, generating an "M"-like feature in the field magnitude as observed, e.g., during the T46 flyby [22]. In such a case, Cassini will detect two distinct enhancements with similar strength which are associated with Titan's magnetic pile-up region. We always consider the strongest field enhancement seen in Titan's interaction region to determine whether Cassini crossed the pile-up region.

(3) Magnetospheric perturbations imposed on the background field (e.g., [16] and [15]) may have a similar magnitude as the pile-up enhancement. For example, during the T89 flyby (see Figure 2.1 (c)), there are some perturbations in $|\vec{B}|$ around 01:03 associated with the motion of Saturn's magnetodisk current sheet, whose magnitude is very close to that of the pile-up signal (denoted by a blue star). The strong perturbations associated with the current sheet oscillation can also be seen in data from the T20 flyby between 08:00 and 14:00 (see Figure 6 in [15]). Thus, a three-step procedure is applied to discriminate between Titan-related signatures and ambient magnetospheric perturbations:

[1] As a baseline to determine the pile-up enhancement, the average magnetospheric field magnitude outside of Titan's interaction region ($|\vec{B}_0|$) is calculated. In addition, $|\mathrm{d}B|$,

which is the value of $|\vec{B}| - |\vec{B}_0|$, is calculated along the entire trajectory within the cube $-10R_T < X, Y, Z < 10R_T$. In analogy to Simon et al. (2010,2013) [15, 22], the typical length of the time intervals considered for computation of the background field is about 90 minutes on either side of the closest approach. Magnetospheric fluctuations that are clearly unrelated to Titan are excluded for calculation of $|\vec{B}_0|$. However, in some cases, $|\vec{B}|$ steadily varies along the trajectory due to large-scale trends in the background field, which could be caused by, e.g., the inhomogeneity of the Saturnian dipole. In these cases, $|\vec{B}_0|$ is determined by a linear fit method which makes $|\vec{B}_0|$ vary along the trajectory between the inbound and outbound regions. The data intervals applied for the $|\vec{B}_0|$ calculation are listed in Table 1.

[2] To determine whether the field enhancements seen near Titan can be unambiguously assigned to the moon's local plasma interaction, we compare the peak field strength in the pile-up region to the magnitude of the strongest ambient field enhancement seen within the $-10R_T < X, Y, Z < 10R_T$ cube, but away from Titan. This strongest magnetospheric field enhancement should be located above an altitude of at least 1 R_T. Below this altitude, the Titan-related perturbations are dominant, regardless of the state of the magnetospheric environment [22]. As can be seen from Figure 2.1 (d), during the T108 flyby, a clear enhancement of $|\vec{B}|$ is superimposed on the quiet background field between 19:35 and 20:08, representing the pile-up region. The pink dashed lines denote a concentric sphere at 1 R_T altitude, i.e., we would search for the strongest ambient field enhancement outside the dashed bars. However, the ambient field during T108 was so quiet that there are no discernible field enhancements outside the dashed bars. In contrast to this, during T88 (see Figure 2.1 (b)), the clear enhancement of $|\vec{B}|$ around 09:03 is associated with the pile-up signature. Between 08:00 and 08:30, there is a distinct peak of $|\vec{B}|$ outside of the pink bars, which is probably associated with a minor fluctuation of the magnetospheric current sheet (as indicated by the simultaneous $|B_Y|$ enhancement).

[3] Finally, we compare the strongest Titan-associated perturbations (named dB_1) against

the maximum level of magnetospheric perturbations (named dB_2), calculate the ratio $|dB_1/dB_2|$. If the ratio $|dB_1/dB_2|$ is larger than 1.5, this implies that the magnetospheric effects are much weaker than the Titan-related pile-up signatures throughout the entire data interval. Thus, we can be sure that the enhancement near Titan is not mainly generated by a magnetospheric fluctuation coincidentally sampled by Cassini.

Cassini's tour in the Saturnian system encompasses 110 flybys that intersect the ramside half space ($X < 0$), 78 of which fulfill the criteria that the maximum Titan-related $|\vec{B}|$ is located at $X <$ 0.5 R_T and within -10 $R_T < X, Y, Z < 10R_T$ cube. Since this paper focuses on the situation when Titan is located inside Saturn's magnetosphere, encounters T32, T42, and T85 are excluded because they occurred in the magnetosheath or even in the solar wind for T85 [25, 26, 27]. Moreover, T54 is also removed as Simon et al. (2010) [15] showed that during this flyby the sweeping of Saturn's magnetodisk current sheet through Titan's immediate environment coincided with Cassini's closest approach to Titan, which completely obscures any signature of draping. For the remaining 74 flybys, 67 flybys satisfy the criterion that the ratio $|dB_1/dB_2|$ should be larger than 1.5. Therefore, 67 flybys in total are relevant for our study, which are listed in Table 1 of the appendix.

In the following, the application of our criteria is demonstrated for two selected flybys (T88 and T108), and we also present one counterexample (T89). The closest approach of T88 was at 1014 km altitude and occurred on 29 November 2012 (13:18 SLT). The T108 encounter took place on 11 January 2015 (23:24 SLT) with a 970 km altitude at the closest approach, while T89 occurred on 17 February 2013 (13:06 SLT) with 1978 km altitude at the closest approach [13].

The dashed half-circle in Figure 2.1 (a) denotes distances below 4 R_T to the center of Titan in the ramside hemisphere, covering the region where the potential signatures of pile-up are expected to be located. During T88, the Cassini spacecraft crossed this shell while approaching from the Saturn-facing and northern side of Titan and moving to the Saturn-averted and southern side. During T89, the spacecraft trajectory was similar to that

of T88. During T108, Cassini entered the ramside pile-up region from the Saturn-facing and southern side of Titan and left it at the Saturn-averted and northern side. Thus, three flybys passed through the half-shell and satisfy the trajectory criterion.

For T88 MAG data are shown in Figure 2.1 (b). The B_Y component displayed fluctuating current sheet features (see also [15] and [17] for the classification of Titan's magnetic environment). Before 08:30 and after 09:10, the B_X component was nearly zero, suggesting that the equatorial portions of the field lines were not lagging significantly behind corotation [18]. At 09:03, Cassini intersected the pile-up region with the strongest enhancement seen at Titan's ramside. Since the background field was mainly oriented southward, the pile-up is mainly visible in the $|B_Z|$ component. The maximum $|\vec{B}|$ is denoted by a blue star and possesses a magnitude of 12.4nT, an altitude of 0.64 R_T and was sampled at position (0.08, -1.64, 0.05) R_T. It fulfills the criterion that the maximum $|\vec{B}|$ should be located in the X < 0.5 R_T half space. The ambient magnetospheric perturbations (caused by the magnetodisk current sheet) generated a second maximum in the inbound region around 08:18, which possesses a $|\vec{B}|$ value of 6.4 nT and an altitude of 4 R_T. The calculated background magnetic field $|\vec{B_0}|$ is approximately 3.6 nT and the green line in the $\mathrm{d}B$ plot (the fifth row) displays the value of the maximum $\mathrm{d}B$ divided by 1.5. Thus, as we can see from the fifth row of Figure 2.1 (b), that secondary maximum (associated with magnetospheric "jitter") does not exceed the threshold displayed by the green line. Therefore, the level of perturbation in Titan's magnetospheric environment is much weaker than the Titan interaction signatures. This makes us confident that the enhancement sampled by Cassini near Titan is actually associated with the pile-up region and contains only minor contributions of magnetospheric fluctuations that may have occurred coincidentally.

The MAG data from T108 are shown in Figure 2.1 (d). Both the inbound and outbound portions of the B_Y component displays a quiet, northern magnetodisk lobe-type field. Additionally, outside of Titan's interaction region, the B_X component was mostly negative with a magnitude of about 2 nT, corresponding to a weak lag of the equatorial

portion of the field behind corotation. Around 19:44, Cassini crossed Titan's magnetic pile-up region with maximum $|\vec{B}|$ marked by a blue star. During this interval, both $|B_Y|$ and $|B_Z|$ increased, since the ambient field was inclined against the north-south direction. The maximum pile-up is located at (0.14, 0.93, 1.1) R_T with an altitude of 0.45 R_T, thereby satisfying our third criterion. Furthermore, we see a slightly asymmetric M-like structure in the field strength, which indicates Cassini coming close to Titan's ionopause. The calculated background magnetic field is $|\vec{B}_0| = 5.6$ nT. Overall, the state of the magnetosphere was extremely quiet during this flyby, with no discernible secondary maxima.

For flyby T89, as shown in Figure 2.1 (c), the fluctuations of the B_Y component detected in the inbound and outbound segments imply that Cassini passed through current sheet fields (see also [17]). At 02:03, the maximum field enhancement near Titan was observed (as denoted by a blue star), located at (-0.01, -2.0, -0.02) R_T with an altitude of 2 R_T and magnitude 10.5 nT. However, there are several peaks in the inbound region which are caused by ambient magnetospheric variability. Around 01:00, the strongest ambient field enhancement with a $|\vec{B}|$ magnitude of 10 nT and an altitude of 6.3 R_T exceeds the green line (again denoting a ratio of 1.5), as shown in the dB plot. This means the magnitude of the ambient magnetospheric perturbations in the immediate vicinity of the moon is comparable to that of the Titan-related signatures, which implies that the near-Titan enhancement could in large portions be unrelated to Titan and not entirely be associated with the pile-up.

The extensions of the pile-up region along the trajectories of T88 and T108 are represented by the light blue bars in Figures 1 (b) and (d). If part of the field enhancement is outside of X < 0.5 R_T, this segment will be removed. The enhanced field downstream of X=0.5 R_T is more likely related to Titan's induced magnetotail. During T88, Cassini entered the pile-up region at 08:59 and exited it at 09:14. For flyby T108, the ambient field is so quiet that the pile-up extension can be easily defined. Cassini entered the pile-up region at 19:38 and exited it around 20:08 where $\mathrm{d}B$ nearly falls to zero.

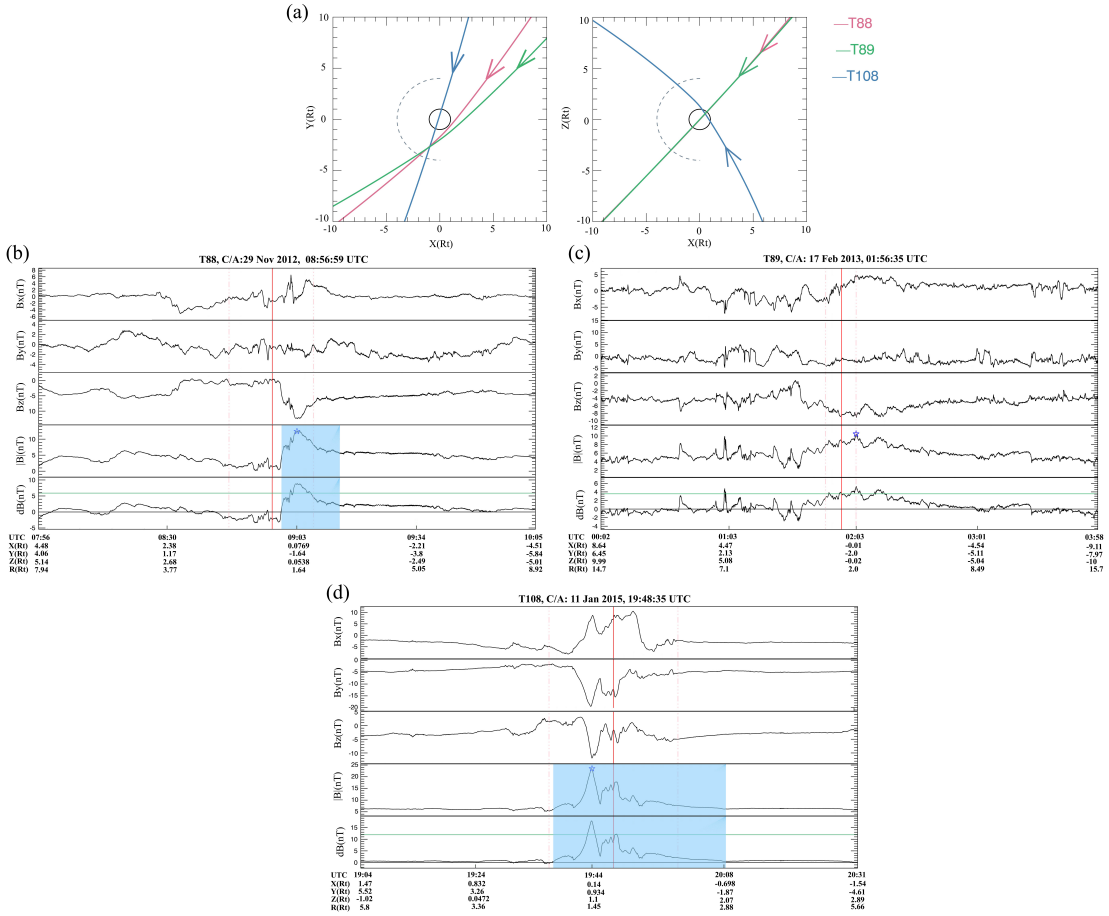

Figure 2.1: (a) Three Titan flybys' trajectories. The red one is the trajectory of T88, the blue one is the trajectory of the T108 flyby and the green is the T89 flyby. (b) MAG data from the T88 flyby. The first to fourth rows are B_X, B_Y, B_Z and $|\vec{B}|$, respectively. The fifth row displays dB, which is the difference between $|\vec{B}|$ and the background magnetic field $|\vec{B}_0|$. The red vertical line denotes the closest approach and the blue star in the fourth row represents the location of maximum $|\vec{B}|$ field pile-up near Titan. (c) MAG data from the T89 flyby. (d) MAG data from the T108 flyby.

CHAPTER 3
RESULTS AND DISCUSSION

3.1 Extension of pile-up region

Based on MAG data from all selected crossings, a profile of Titan's ramside pile-up region during the Cassini era has been generated. This profile displays the segments along the flyby trajectories during which Cassini was located inside the region of pile-up field lines, as shown in Figures 3.1 (a)-(d). In the following, we will investigate how the observed extensions of the pile-up region depend on Titan's orbital position (given by the local time) and ambient magnetospheric environments.

3.1.1 Extension of pile-up region at different Saturn local times

Figures 3.1 (a)-(d) show the projections of the observed pile-up signatures onto the X-Y and X-Z planes of the Titan Interaction System when Titan is located in the dayside and nightside sectors of Saturn's magnetosphere, respectively. Figure 3.1 (e) shows the distribution of 67 selected flybys in the different sectors of Titan's orbit around Saturn, defined by the Saturnian local time (SLT). As can be seen from figure 3.1 (e), we divide Titan's orbit into 4 segments, which are 03:00-09:00, 09:00-15:00, 15:00-21:00, and 21:00-03:00 SLT. However, the only two sectors considered by our study are 09:00-15:00 (around noon) and 21:00-03:00 (around midnight). When Titan is in the 09:00-15:00 SLT, the solar radiation is nearly perpendicular to the co-rotation direction, pointing to Saturn; and in the 21:00-03:00 SLT, the radiation is again perpendicular to the co-rotation direction but points away from Saturn. We have 30 flybys in the 09:00-15:00 SLT and 27 flybys in the 21:00-03:00 SLT, whereas there are only 3 flybys in the dawn (03:00-09:00 SLT) and 7 flybys in the dusk (15:00-21:00 SLT) sectors. These two sectors are therefore not covered well

enough for statistically meaningful conclusions. Therefore, we only compare the dayside (09:00-15:00 SLT) and nightside (21:00-03:00 SLT) sectors when investigating the structure of Titan's pile-up region at different orbital positions. Different orbital positions result in different illumination angles of Titan with respect to the co-rotational flow direction, which might cause a stronger mass loading on the illuminated side affecting the magnetic field. When Titan is in the dayside or nightside sectors of Saturn's magnetosphere, the Saturn-averted side ($Y < 0$) or Saturn-facing side ($Y > 0$) are exposed to solar radiation, shifting the region of strongest mass loading. It is important to notice that when Titan is in the nightside sector, it was *never* encountered by Cassini while the geometric shadow of Saturn [13].

As we can see from figures 3.1 (a) and (c), the projections of the pile-up profiles in both, the dayside and nightside sectors are much more extended on the Saturn-averted side ($Y < 0$) where the convective electric field has a strong component away from Titan. This disparity is likely associated with the asymmetry caused by the large gyroradii of pick-up ions, as shown by numerical simulations (e.g., [8]). As can be seen in figure 3.1 (a) when Titan is in the dayside sector of Saturn's magnetosphere, the pile-up region extends into the Saturn-facing hemisphere no farther than $Y \approx 2R_T$, while it penetrates into the Saturn-averted side no farther than $Y \approx -4.8R_T$. In figure 3.1 (c), we can see that the pile-up can penetrate into the Saturn-facing hemisphere to $Y \approx 2.5R_T$, but it penetrates into the Saturn-averted hemisphere no farther than $Y \approx -4.5R_T$. The observed extension of the pile-up region on the Saturn-averted side is similar to the gyroradii of the pick-up ions: for instance, the cycloidal arcs of N_2^+ possess an extension of about 5.4 R_T along the direction of $\vec{E_0}$. This asymmetry was also detected in the density of escaping ions by the Radio and Plasma Wave Science (RPWS) Langmuir probe (LP) sensor during the TB flyby, showing an extended mass-loading region on the Saturn-averted side of Titan [24]. In north-south direction, when Titan is in the dayside sector of Saturn's magnetosphere the pile-up extends from $Z \approx -3$ R_T to 4 R_T, and when in the nightside sector the pile-up is

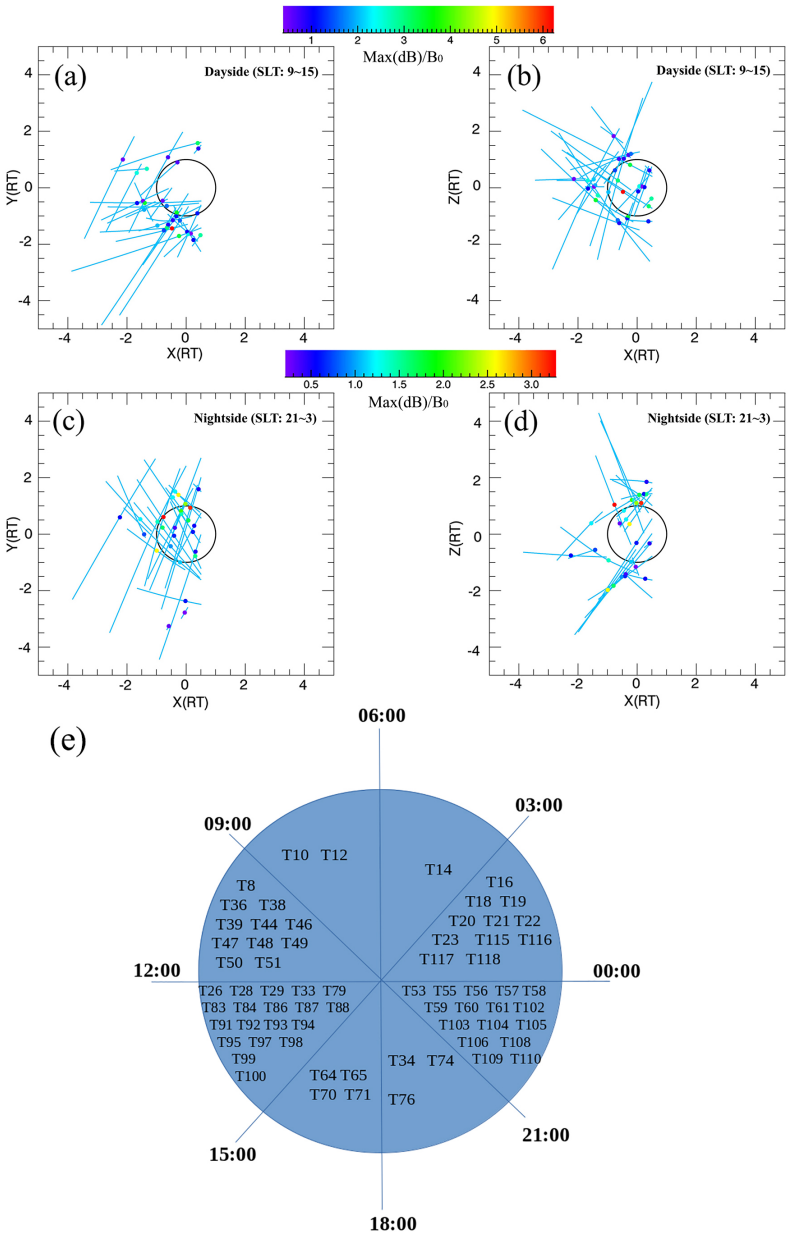

Figure 3.1: (a) The blue lines are the observed extensions of the pile-up region when Titan is in the dayside sector of Saturn's magnetosphere (SLT: 09:00-15:00), projected onto the X-Y plane. The dots along the trajectories are the locations of the maximum $|\vec{B}|$ for each flyby, color-coded by the ratio between maximum field strength and the background field. (b) The projection of the observed pile-up region onto the X-Z plane when Titan is in the dayside sector of Saturn's magnetosphere. (c) Projection onto the X-Y plane when Titan is in the nightside sector of Saturn's magnetosphere (SLT: 21:00-03:00). (d) Projection onto the X-Z plane when Titan is in the nightside sector of Saturn's magnetosphere. (e) The flyby distribution depending on the SLT.

from $Z \approx -3.5$ to 4 R_T, which do not reflect a clear asymmetry between the northern and southern hemispheres.

In general, the observed pile-up extensions are nearly independent of Titan's orbital position. These results are consistent with the study of Ledvina et al. (2012) [10], who modeled Titan's plasma interaction under three different solar illumination angles, i.e., when Titan is located at 06:00, 12:00 and 18:00 SLT. These authors showed the identical extension and location of the pile-up and the same asymmetry about the flow axis for different orientations of the dayside ionosphere. In figure 3.1 (c), we find that the extension of the pile-up in the nightside sector is slightly (0.5 R_T) more extended to the Saturn-facing side than in the dayside sector. Apart from observational bias due to the limited number of events, this slight disparity may be caused by the fact that in the nightside sector, Titan's $Y > 0$ half space (which contains the trajectories of the escaping ions) is illuminated, leading to a more extended mass loading region in that hemisphere. An anti-Saturnward rotation of the upstream plasma flow in the nightside sector [28] might contribute to this small discrepancy as well by rotating the pile-up slightly to the Saturn-facing side.

3.1.2 Extensions of Titan's magnetic pile-up region when exposed to different Saturnian magnetospheric environments

Since Saturn's warped and highly dynamic magnetodisk strongly affects Titan's magnetic environment, Simon et al. (2010,2013) [15, 22] and Kabanovic et al. (2007) [17] have categorized the moon's ambient magnetic environment during each Cassini flyby as current sheet, lobe-like, magnetosheath, or an admixture of these regimes. Rymer et al. (2009) [29] and Smith & Rymer (2014) [30] used the electron spectra to characterize the magnetospheric upstream regimes into plasma sheet, lobe-like, magnetosheath and bimodal. However, the Cassini Plasma Spectrometer has been turned off since 2 June 2012, which means the classifications by Rymer et al. (2009) [29] and Smith & Rymer (2014) [30] are available only for a subset of all flybys. Therefore, we apply the available magnetic field

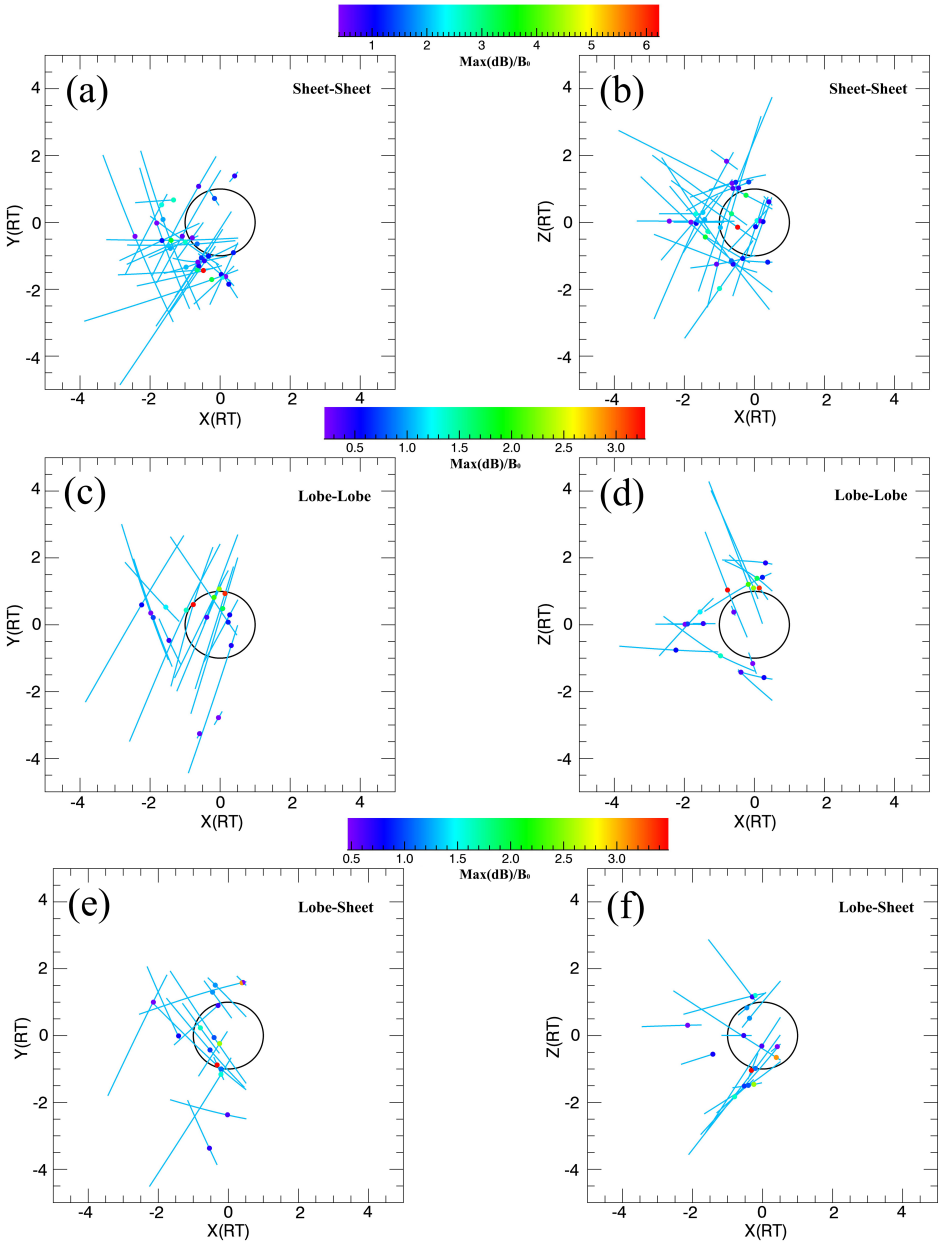

Figure 3.2: The pile-up extensions under different upstream conditions, projected onto the X-Y and X-Z planes. The magnetospheric environments are characterized by the classification of Simon et al. (2010,2013) [15, 22]. Sheet-Sheet means that the current sheet environment was observed during both, the inbound and outbound segment of the flyby. Lobe-Lobe means that during the inbound and outbound segments of the flyby, Cassini detected lobe-type fields with the same orientation of B_Y. Lobe-Sheet means that the inbound and outbound segments of the flyby revealed different magnetospheric environments, i.e., either the inbound segment is lobe type and the outbound segment is the current sheet type or the inbound segment is the current sheet type and the outbound segment is the lobe type.

classifications to investigate the effect of different Saturnian magnetospheric environments on Titan's pile-up region.

In the studies of Simon et al. (2010,2013) [15, 22], the ambient magnetospheric field regime at Titan was classified into: (1) magnetodisk current sheet type (Sh) when the field points mainly in north-south direction with small $|B_Y|/|\vec{B}|$ and the B_Y component has strong fluctuations (on time scales way below 30 minutes) due to the oscillating magnetodisk current sheet; (2) northern/southern magnetodisk lobe type (L^N/L^S) when the field is radially stretched with a large B_Y component and rather weak fluctuations within time intervals of 30 minutes; (3) northern/southern lobe with brief occurrences of current sheet fields (L^N_{Sh}/L^S_{Sh}) when the ratio of fluctuation of B_Y and the average magnetic field magnitude is larger than 0.05 but smaller than 0.2; (4) magnetosheath type (Msh) when Cassini was located outside of Saturn's magnetosphere.

Based on the expected similarity of the plasma conditions in the two magnetodisk lobes and to obtain a sufficient number of data points in each category, we only classify the ambient magnetic field conditions during a certain flyby into lobe type (symbol L, including L^N, L^S, L^N_{Sh} as well as L^S_{Sh}), and current sheet type (symbol Sh). The symbols $L-L$ and $S-S$ refer to flybys where the magnetic environments in both, the inbound and outbound segments are L (lobe type) or S (current sheet type), respectively. The abbreviations $L-S$ means that the inbound and outbound types are different, e.g., the inbound environment is L while the outbound environment is Sh *and vice versa*. Our set of selected events encompasses 17 flybys that took place in an $L-L$ environment, 16 flybys in an $L-S$ environment, and 30 flybys with an $S-S$ environment. The "reduced" categorizations used here are the same as applied by [17].

Figures 3.2 (a)-(f) show the observed extensions of the pile-up region when Titan is exposed to different magnetic environments. In the $S-S$ regime, B_Z is the predominant component of the background field and thus, the associated convective electric field is nearly aligned with the $(+Y)$ axis, which implies that plane containing the pick-up cycloids

is very close to the X-Y plane. As can be seen from figure 3.2 (a), there is a clear asymmetry in the extension of the pile-up between the Saturn-averted and the Saturn-facing sides. The observed pile-up region extends to the Saturn-averted side no farther than $Y \approx -5$ R_T, while it penetrates into the Saturn-facing hemisphere only up to $Y \approx 2R_T$. As can be seen in figure 3.2 (b), the data do not reveal any obvious asymmetry between the northern and southern hemispheres. For the $L - L$ environment, the background magnetic field is radially stretched with a rather large B_Y (either positive or negative) component. However, Arridge et al. (2011) [31] showed that the convective electric field still points into the $Y < 0$ half-space. The plane of gyration is lifted out of Titan's equatorial plane (Z=0) into the northern or southern hemisphere. As shown in figure 3.2 (c), the pile-up region in this magnetospheric regime extends to the Saturn-facing side no farther than Y=3 R_T along the positive Y direction, and penetrates into the Saturn-averted hemisphere up to $Y \approx -4.5R_T$. Though the coverage is uneven due to only 17 flybys in the $L - L$ category, this slight disparity might still imply an asymmetry between the Saturn-averted and the Saturn-facing sides of the pile-up region when Titan is exposed to the $L - L$ environment. As shown in figure 3.2 (d), the pile-up seems to be more extended into Titan's northern hemisphere than into the southern hemisphere. The observed extensions of the pile-up extended to the northern hemisphere up to $Z \approx 4R_T$, and extended to the southern hemisphere only up to $Z \approx -2.5R_T$. Two flybys (whose observed pile-up extensions penetrated into the northern hemisphere up to 4 R_T as shown in figure 3.2 (d)), T104 and T105, crossed Titan when the moon was exposed to the northern lobe field [17]. Therefore, the convective electric field during these two encounters possessed a $+Z$ component instead of pointing precisely in $-Y$ direction, thereby lifting the pick-up tail toward the north and leading to the detection of an extended pile-up in the northern hemisphere. For the mixed regime, $L - S$, the observed pile-up extension also shows an asymmetry between the Saturn-facing and Saturn-averted sides, and is nearly symmetric between the northern and southern hemisphere. These imply that the expected asymmetries in ionospheric ion escape do indeed

manifest in the magnetic field, as suggested by various models of the Titan interaction.

In conclusion, the different magnetospheric environments do not appear to change the extension of the pile-up in a clearly discernible way, based on MAG data from the entire Cassini era. However, the extension of the pile-up region should respond to different magnetospheric environments. When Titan is embedded in the magnetodisk current sheet, the background field is nearly dipolar and the incident plasma consists mainly of heavy ions with a high value of beta, which leads us to expect a pile-up region that is more compressed than that in the magnetodisk lobes. When Titan is embedded in the lobe environment, the incident plasma is dilute and consists mainly of light ions with a low beta value [19, 20]. Therefore, we expect a pile-up region that is less compressed than in the magnetodisk current sheet. These expected differences in the structure of the pile-up region in the current sheet and lobe-type regimes were probably not recorded due to the (still) rather sparse data coverage in each of the three magnetospheric regimes considered here.

3.2 Altitude profile of the pile-up region

To study the strength of field pile-up as a function of altitude, each of the observed pile-up segments (as shown in figure 3.2) is sliced by 25 concentric annuli with a width of 0.1 R_T and origin at the center of Titan. Since the Cassini spacecraft was closest to Titan during T70 with an altitude of 0.3 R_T, the smallest annulus starts at 0.3 R_T altitude. Above the altitude of about 2.8 R_T, there is not discernible pile-up. Hence, the radius of the largest annulus has a range of 2.7-2.8 R_T. The ratio of maximum $|\vec{B}|$ and the background field $|\vec{B_0}|$ is calculated for each observed pile-up segment within each annulus it crosses. In each annulus, we take the average of these ratios as an indicator of the pile-up strength, either for all flyby segments within the annulus or only for those from flybys that meet additional criteria (e.g., dayside sector flybys, lobe-lobe flybys, etc).

Figures 3.3 (a) and (b) display the altitude profiles of the pile-up strength with the associated standard deviations in the dayside and nightside sectors of Saturn's magnetosphere,

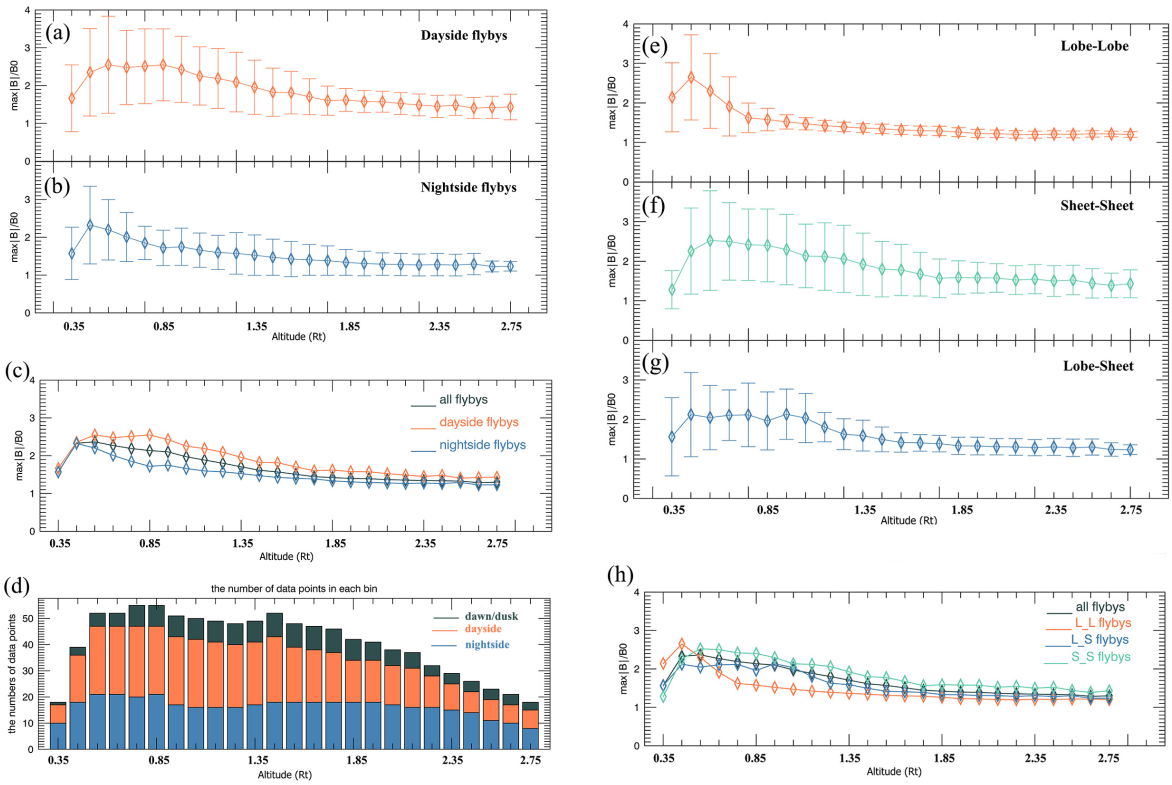

Figure 3.3: Panels (a) and (b) show the averaged pile-up strength with the associated standard deviation when Titan was in the dayside and nightside sectors (09:00-15:00 SLT and 21:00-03:00 SLT) of Saturn's magnetosphere, respectively. Panel (c) shows the comparison of the averaged pile-up strength in the dayside and nightside sectors as well as all sectors combined. The orange line represents the pile-up strength when Titan was in the dayside sector of Saturn's magnetosphere. The blue line displays the pile-up strength when Titan was in the nightside sector of Saturn's magnetosphere. The black line shows the average altitude profile of all observed pile-up signatures. Panel (d) displays the number of data points in each bin. The heights of the blue and orange bars represent the number of data points when Titan was in the nightside and dayside sectors, respectively. The height of the grey bar shows the number of data points that were obtained for the dawn/dusk sectors (03:00-09:00 SLT/ 15:00-21:00 SLT). Panels (e)-(g) show the averaged pile-up strength with the standard deviation when Titan is embedded in the lobe-lobe, sheet-sheet, and lobe-sheet environments, respectively (using the categorizations from [17]). Panel (h) displays the comparison of the averaged altitude profiles of the pile-up region when Titan was embedded in different Saturnian magnetospheric environments.

respectively. When Titan was in the dayside sector of Saturn's magnetosphere, the pile-up strength increases from 0.35 R_T upward, and reaches a peak value of around 2.5 B_0 at altitudes between 0.45 R_T to 0.95 R_T. Above these altitudes, the pile-up gradually decreases.

When Titan was in the nightside sector, the maximum pile-up strength was observed around 0.45 R_T. The field strength sharply drops from 0.45 R_T to 0.85 R_T, and then slowly decreases. Overall, the pile-up profiles of the dayside and nightside categories are within each other's range (considering the error bars), implying that the pile-up strength is independent of Titan's position along its orbit around Saturn. However, both profiles still display quantitatively different features. In figure 3.3 (c), we find that the pile-up (independent of the magnetospheric environment category) in the dayside sector is stronger than that in the nightside and all flybys categories, especially between altitudes of 0.55 R_T to 1.65 R_T. When Titan is in the dayside sector, it is mostly embedded in a broad magnetodisk current sheet populated by heavy ions. Therefore, the upstream ram pressure is higher than that in the nightside sector where the moon is more frequently located in the lobe-type regime populated by light ions [19, 20]. Hence, when Titan is in the dayside sector, the magnetic field in the pile-up region is likely to be stronger than the field enhancement when Titan is in the nightside sector due to the elevated ram pressure of the upstream plasma. However, as also discussed in section 3.1, this effect is rather quantitative in nature and Cassini data do not reveal a significant local time dependence of Titan's ramside magnetic barrier.

Furthermore, the field strength at low altitudes never drops to zero although the pile-up weakens around 0.35 R_T altitude, which might imply that this altitude is close to the average position of the ionopause. Below altitudes of 0.62 R_T (1600 km), the magnetic field can contain contributions of fossil fields [4, 32], data collected in this altitude range may not show the response of the pile-up to the current ambient magnetospheric field.

Figures 3.3 (e)-(g) show the altitude profiles of the pile-up strength with the associated standard deviations in different magnetospheric environments: lobe-lobe, sheet-sheet, and lobe-sheet, respectively [17]. The pile-up strength in the lobe-lobe category exhibits the sharpest peak from 0.35 R_T to 0.75 R_T. In the sheet-sheet and lobe-sheet categories, the peaks of pile-up profiles are broader. In figure 3.3 (h), at 0.35 R_T altitude, the pile-up strength in the lobe-lobe category is stronger than in the sheet-sheet and lobe-sheet cat-

egories. Additionally, above an altitude of 0.65 R_T, the averaged pile-up strength in the lobe-lobe environment is smaller than in the other two categories. In particular, around an altitude of 0.85 R_T, the normalized field strength is about 1.6 in the lobe-lobe category and 2.4 in the sheet-sheet category. Thus, the increased compression of the ramside magnetic field in the sheet-sheet environment may have a discernible impact on the observable pile-up signatures. Modeling results (e.g., [7]) suggest the maximum pile-up in Saturn's magnetodisk lobes to be at least a factor of 2 weaker than in the current sheet. It could be the uneven coverage with flyby segments that makes the observable impact of this effect appear weaker than it is in reality.

Despite this disparity, it is important to note that the altitude profiles of the pile-up with their corresponding standard deviations in different magnetospheric environments are included within each other's range, i.e., the altitude profile of the pile-up strength changes between the different magnetospheric environments only quantitatively but not qualitatively. This stable picture of the ramside features in Titan's induced magnetosphere is consistent with the study of Simon et al. (2013) [22], who found that the moon's wakeside magnetotail structure is very "robust" against the continuous changes in the magnetospheric environment. The notion of steady-state field line draping is able to explain the magnetic field data from over 60% of the relevant tail crossings, even when Titan is embedded in the perturbed current sheet fields.

Figures 3.4 (a) and (b) show the altitude profiles of the pile-up strength in the $Y > 0$ and $Y < 0$ hemispheres, respectively. In both hemispheres, the pile-up strength drastically increases from 0.35 R_T to 0.45 R_T. The field strength again starts to drop above altitudes of 0.65 R_T in the $Y > 0$ hemisphere, but in the $Y < 0$ hemisphere, it begins to decrease at an altitude of 0.75 R_T. Figure 3.4 (c) reveals that the normalized field magnitudes in the $Y < 0$ hemisphere are about 30-40% larger than those in the $Y > 0$ hemisphere (between 0.65 R_T and 2.55 R_T). This asymmetry could be caused by the large ion gyroradii, leading a slightly stronger pile-up on the Saturn-averted side. Taking into account the large standard

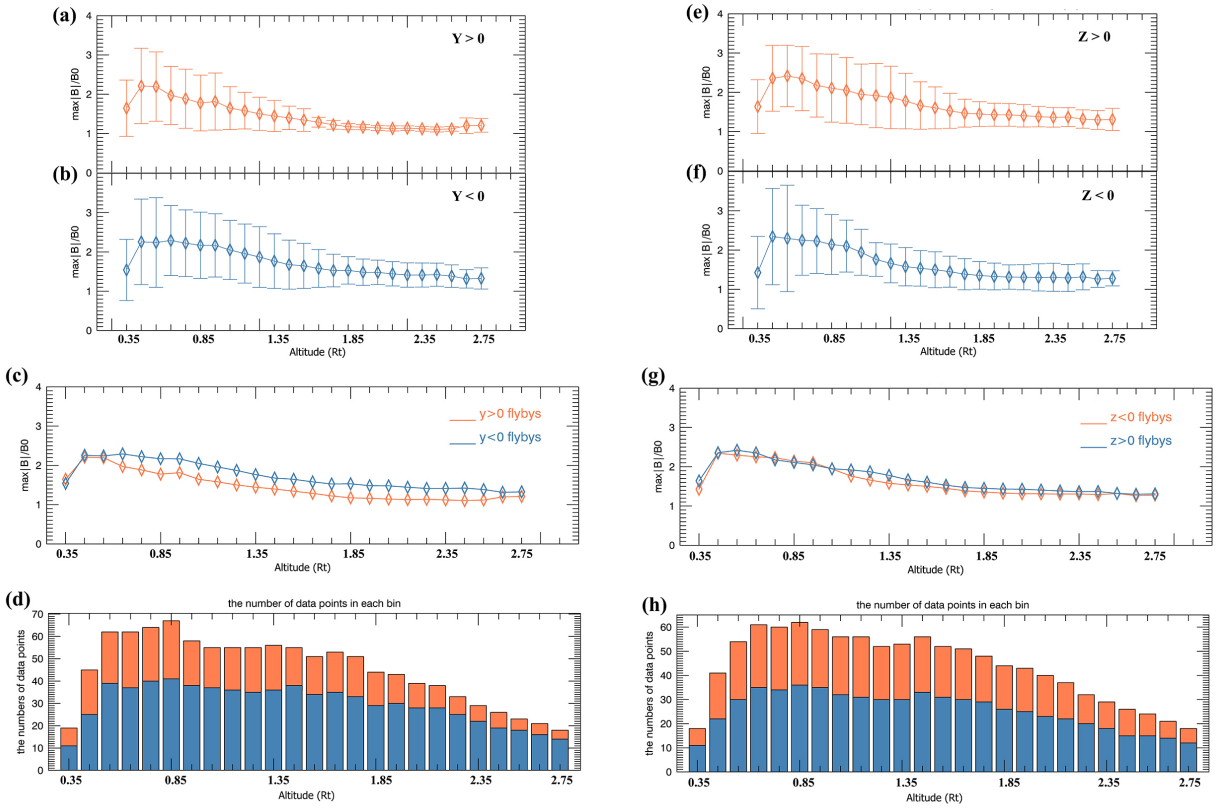

Figure 3.4: Panels (a) and (b) show the averaged pile-up strength with the corresponding standard deviation in the $Y > 0$ and $Y < 0$ hemispheres, respectively. Panel (c) shows the comparison of the averaged pile-up strengths in both half spaces. The orange line represents the pile-up strength in the Saturn-facing hemisphere. The blue line displays the pile-up strength in the Saturn-averted hemisphere. Panel (d) displays the number of data points in each altitude bin. The heights of blue and orange bars represent the number of data points obtained for the Saturn-averted and Saturn-facing sides, respectively. Panels (e) and (f) show the averaged pile-up strength with the associated standard deviation in the northern and southern hemispheres, respectively. Panel (g) displays the comparison of the averaged pile-up strengths seen north and south of Titan. Panel (h) shows the number of data points in each bin. The heights of blue and orange bars represent the number of data points obtained for the northern and southern hemispheres, respectively.

deviations, it is important to note that the pile-up strength is not significantly affected by the expected hemispherical asymmetries of the pick-up ion on the pick-up ion trajectories. However, models (e.g., [7]) suggest the asymmetries in the magnetic field to be much stronger. It could be that, at the low altitudes covered by most of the Cassini flybys near Titan, these asymmetries are not yet fully developed and become more apparent at larger distances to the moon. However, at higher altitudes, data coverage quickly becomes too

sparse to draw meaningful conclusions.

Figures 3.4 (e) and (f) show the altitude profiles of the pile-up strength in the northern ($Z > 0$) and southern ($Z < 0$) hemispheres, respectively. The pile-up strengths in both hemispheres reach their maximum values at low altitudes (0.45-0.55 R_T). As can be seen from figure 3.4 (g), the pile-up strength is nearly symmetric between the northern and southern hemispheres. However, a north-south asymmetry of the pile-up should be caused by the sweep-back of the field lines in the magnetodisk lobes [18, 8]. When Titan is embedded in the current sheet, there is no sweep-back. Therefore, the pile-up should display a north-south asymmetry when Titan is embedded in the northern/southern magnetodisk lobe, and this asymmetry should be discernible in the current sheet regime. Although several flybys (e.g., T104 and T105) reveal a north-south asymmetry of the draping when Titan is exposed to lobe-type fields (see figure 3.2 (d)), this effect seems to average out when considering all the events.

Figures 3.4 (a) and (b) show the altitude profiles of the pile-up strength in the $Y > 0$ and $Y < 0$ hemispheres, respectively. In both hemispheres, the pile-up strength drastically increases from 0.35 R_T to 0.45 R_T. The field strength again starts to drop above altitudes of 0.65 R_T in the $Y > 0$ hemisphere, but in the $Y < 0$ hemisphere, it begins to decrease at an altitude of 0.75 R_T. Figure 3.4 (c) reveals that the normalized field magnitudes in the $Y < 0$ hemisphere are about 30-40% larger than those in the $Y > 0$ hemisphere (between 0.65 R_T and 2.55 R_T). This asymmetry could be caused by the large ion gyroradii, leading a slightly stronger pile-up on the Saturn-averted side. Taking into account the large standard deviations, it is important to note that the pile-up strength is not significantly affected by the expected hemispherical asymmetries of the pick-up ion on the pick-up ion trajectories. However, models (e.g., [7]) suggest the asymmetries in the magnetic field to be much stronger. It could be that, at the low altitudes covered by most of the Cassini flybys near Titan, these asymmetries are not yet fully developed and become more apparent at larger distances to the moon. However, at higher altitudes, data coverage quickly becomes too

sparse to draw meaningful conclusions.

Figures 3.4 (e) and (f) show the altitude profiles of the pile-up strength in the northern ($Z > 0$) and southern ($Z < 0$) hemispheres, respectively. The pile-up strengths in both hemispheres reach their maximum values at low altitudes (0.45-0.55 R_T). As can be seen from figure 3.4 (g), the pile-up strength is nearly symmetric between the northern and southern hemispheres.

However, a north-south asymmetry of the pile-up should be caused by the sweep-back of the field lines in the magnetodisk lobes [18, 8]. When Titan is embedded in the current sheet, there is no sweep-back. Therefore, the pile-up should display a north-south asymmetry when Titan is embedded in the northern/southern magnetodisk lobe, and this asymmetry should be discernible in the current sheet regime. Although several flybys (e.g., T104 and T105) reveal a north-south asymmetry of the draping when Titan is exposed to lobe-type fields (see figure 3.2 (d)), this effect seems to average out when considering all the events.

CHAPTER 4
CONCLUSION

In this study, we have conducted a systematic investigation of Cassini MAG observations from all flybys crossing Titan's ramside magnetic pile-up region. Our study reveals the properties of the extension and strength of magnetospheric field line pile-up at Titan.

The extension of the pile-up region is much larger on the moon's Saturn-averted side ($Y < 0$). This asymmetry of the pile-up region is likely caused by the large gyro-radii of pick-up ions. Furthermore, the observed extensions of the pile-up region are nearly independent of Titan's orbital position, although the solar illumination angles are different. However, when Titan is in the nightside sector, the pile-up region seems to be slightly more extended to the Saturn-facing side than in the dayside sector. This difference could be caused by a stronger mass loading region in the $Y > 0$ hemisphere due to higher EUV ionization rates, or a possible anti-Saturnward rotation of the upstream plasma flow in the nightside sector [28]. Between the different magnetospheric environments to which Titan is exposed, the pile-up extension does not differ in a clearly discernible way, which might partially be due to the sparse data coverage.

The altitude profiles of the pile-up strength all show a decrease around 0.35 R_T. However, the field never drops to zero, i.e., there is no clear signature of Titan's (magnetic) ionopause discernible in Cassini MAG data. Considering the error bars, the altitude profile of the pile-up seems to be independent of Titan's position along its orbit around Saturn and the magnetospheric environment category. Quantitatively, when Titan is in the dayside sector, the pile-up is stronger than that in the nightside. This is because in the dayside sector of Saturn's magnetosphere, the moon is embedded in the broad magnetodisk current sheet [17], which is populated mainly by heavy ions [19, 20] causing an elevated ram pressure of the upstream plasma. This result is consistent with our finding that the pile-up strength

in the lobe-lobe environment is weaker than in the other two categories (sheet-sheet and lobe-sheet). Between the Saturn-facing ($Y > 0$) and Saturn-averted ($Y < 0$) hemispheres, the altitude profile of the pile-up strength is not significantly affected by the expected hemispherical asymmetries of the pick-up ion trajectories. These asymmetries may not yet be discernible at the low altitudes where the Cassini flybys provide sufficient data coverage, and the data coverage is too sparse at higher altitudes. The altitude profiles obtained for the northern and southern hemispheres show that the pile-up region is nearly symmetric between the $Z > 0$ and $Z < 0$ hemispheres. Although a north-south asymmetry should exist when Titan is exposed to lobe-type fields, this effect seems to be averaged out when considering all the events (that include flybys from both, the northern and the southern magnetodisk lobe).

Appendices

APPENDIX A

TABLE OF SELECTED FLYBYS

The columns from left to right in Table 1 are: (1)Selected Titan flybys of the Cassini Mission. The asterisk means that B_0 of this flyby has been calculated by the linear fit method. (2) Date and time of the closest approach of each flyby. (3) Saturn local time. (4) Ambient magnetospheric environments (these classifications obtained from [17]). The asterisk means that the classifications are not available due to either the data gap or the unclassified environment [15, 17]. (5) Magnitude of the background magnetic field. (6) Maximum $|\vec{B}|$ (the pile-up related). (7) Ratio of maximum $|\vec{B}|$ (the pile-up related) and the background field $|\vec{B}_0|$. (8) Magnitude of the background magnetic field calculated before the closest approach. The symbol "-" means that we do not use the magnetic field in the inbound to calculate the background field due to either the data gap or the intense perturbation of the magnetic field. (9) Time intervals we used to calculate $|\vec{B}_0|$ in the inbound. (10) Magnitude of the background magnetic field calculated after the closest approach. The symbol "-" means that we do not use the magnetic field in the outbound to calculate the background field due to either the data gap or the intense perturbation of the magnetic field. (11) Time intervals we used to calculate $|\vec{B}_0|$ in the outbound.

Table A.1: Selected Titan flybys of the Cassini mission for the study of the pile-up region. Details are discussed in the Appendix.

Flyby	Date and Time of C/A(UTC)	SLT(h)	Ambient Environment	B_0 (nT)	B_{max} (nT)	B_{max}/B_0	inbound B_0 (nT)	inbound range	outbound B_0 (nT)	outbound range
$T8*$	2005 OCT 28 (301), 04:08:07	9.3	L-L	4.4	6.3	1.4	3.9	03:02:57-03:52:57	4.8	04:33:54-04:58:54
$T10$	2006 JAN 15 (015), 11:41:25	8.5	L-S	5.2	8.8	1.7	5.2	08:53:11-10:23:14	-	-
$T12*$	2006 MAR 19 (078),00:05:55	6.4	L-L	6.4	7.7	1.2	6.2	23:12:25-23:27:25	6.6	01:05:05-01:30:05
$T14$	2006 MAY 20 (140), 12:18:11	4.4	L-L	4.7	8.2	1.7	4.7	10:26:23-11:31:22	-	-
$T16*$	2006 JUL 22 (203), 00:25:26	2.4	*	3.7	9.4	2.5	2.8	23:01:23-23:26:23	4.7	01:13:56-01:38:56
$T18$	2006 SEP 23 (266), 18:58:48	2.3	L-L	4.7	7.6	1.6	5.2	16:51:36-18:21:36	4.2	20:09:46-21:39:46
$T19$	2006 OCT 09 (282), 17:30:07	2.2	L-S	5.7	12.7	2.2	6.1	15:58:52-17:13:52	5.4	18:17:55-19:47:55
$T20$	2006 OCT 25 (298), 15:58:07	2.2	L-S	6.2	9.0	1.5	-	-	6.2	16:36:19-18:08:06
$T21$	2006 DEC 12 (346), 11:41:31	2.1	L-L	5.8	12.8	2.2	5.6	09:51:00-11:21:07	6.1	12:44:22-14:15:04
$T22$	2006 DEC 28 (362), 10:05:21	2.0	L-S	5.1	11.3	2.2	5.5	06:43:18-08:13:18	4.7	12:05:37-13:35:37
$T23$	2007 JAN 13 (013), 08:38:31	2.0	*	4.0	14.4	3.6	2.5	05:28:20-06:58:20	5.5	09:33:39-11:03:42
$T26$	2007 MAR 10 (069), 01:49:00	13.8	L-S	4.3	7.1	1.7	4.3	23:47:38-01:17:38	-	-
$T28$	2007 APR 10 (100), 22:57:59	13.7	S-S	4.6	8.4	1.8	-	-	4.6	00:49:23-02:39:23
$T29*$	2007 APR 26 (116), 21:32:58	13.7	S-S	6.2	9.0	1.5	4.5	20:24:19-20:40:59	6.8	22:09:22-22:26:02
$T33$	2007 JUN 29 (180), 16:59:45	13.6	S-S	4.4	15.4	3.5	4.8	14:13:56-15:43:56	4.0	18:27:00-19:57:00
$T34$	2007 JUL 19 (200), 01:11:20	18.8	S-S	3.7	10.7	2.9	3.9	22:27:08-00:37:08	3.3	01:49:22-03:19:25
$T36$	2007 OCT 02 (275), 04:42:43	11.5	S-S	5.8	12.6	2.2	5.8	01:55:45-03:25:45	-	-
$T38$	2007 DEC 05 (339), 00:06:49	11.4	S-S	5.8	10.8	1.9	-	-	5.8	01:31:00-03:01:00
$T39$	2007 DEC 20 (354), 22:57:55	11.4	S-S	7.8	16.7	2.1	9.3	20:49:34-22:19:34	6.3	00:25:20-01:55:20
$T44$	2008 MAY 28 (149), 08:24:32	10.9	S-S	3.9	16.6	4.3	-	-	3.9	09:53:59-11:23:59
$T46$	2008 NOV 03 (308), 17:35:22	10.5	L-S	3.0	12.1	4.0	3.0	14:33:43-16:03:43	-	-
$T47$	2008 NOV 19 (324), 15:56:27	10.4	S-S	2.2	15.6	7.1	2.2	12:54:52-14:24:52	2.1	17:26:49-18:56:49
$T48$	2008 DEC 05 (340), 14:25:45	10.4	S-S	2.2	8.8	4	2.8	12:14:37-13:44:37	1.6	15:56:14-17:26:14
$T49$	2008 DEC 21 (356), 12:59:52	10.3	S-S	4.5	19.5	4.3	5.3	09:50:34-11:20:34	3.7	14:32:27-16:02:27
$T50$	2009 FEB 07 (038), 08:50:51	10.2	S-S	3.4	12.6	3.7	3.6	06:38:44-08:08:44	3.2	09:39:05-11:09:05
$T51$	2009 MAR 27 (086), 04:43:36	10.1	S-S	3.6	9.3	2.6	2.7	01:49:38-03:19:38	4.4	06:13:18-07:43:18
$T53$	2009 APR 20 (110), 00:20:45	22.0	L-S	4.3	7.0	1.6	-	-	4.3	01:57:59-03:28:06
$T55$	2009 MAY 21 (141), 21:26:41	22.0	S-S	2.9	10.2	3.5	2.2	18:39:18-20:09:18	4.1	22:00:21-23:00:21
$T56$	2009 JUN 06 (157), 20:00:00	21.9	L-S	3.7	7.8	2.1	-	-	3.7	21:09:03-22:39:03
$T57*$	2009 JUN 22 (173), 18:32:35	21.9	L-S	4.3	8.4	2.0	3.3	17:11:50-18:01:50	5.3	19:15:41-20:05:41
$T58*$	2009 JUL 08 (189), 17:04:03	21.8	L-S	4.2	11.0	2.6	4.9	15:30:21-16:03:41	3.7	18:04:46-18:54:46
$T59$	2009 JUL 24 (205), 15:34:03	21.8	L-S	5.5	9.1	1.7	-	-	5.5	16:13:14-17:43:14
$T60$	2009 AUG 09 (221), 14:03:53	21.7	S-S	3.1	7.6	2.5	2.8	12:01:43-13:33:33	3.7	14:34:47-15:35:10
$T61$	2009 AUG 25 (237), 12:51:37	21.7	L-S	5.4	9.4	1.7	-	-	5.4	13:28:38-14:58:38
$T64$	2009 DEC 28 (362), 00:16:58	17.0	S-S	2.4	5.4	2.3	-	-	2.4	00:57:04-02:28:17
$T65$	2010 JAN 12 (012), 23:10:35	16.9	L-S	4.5	16.0	3.6	5.5	21:02:41-22:32:41	3.5	00:02:57-01:32:57
$T70$	2010 JUN 21 (172), 01:27:43	16.1	S-S	5.5	8.1	1.5	5.0	22:27:01-23:58:50	6.0	02:58:18-04:28:25
$T71$	2010 JUL 07 (188), 00:22:45	16.1	S-S	2.9	4.6	1.6	-	-	2.9	01:03:35-02:33:35
$T74$	2011 FEB 18 (049), 16:04:11	20.6	S-S	4.0	5.7	1.4	-	-	4.0	16:41:56-17:23:36
$T76*$	2011 MAY 08 (128), 22:53:44	19.8	S-S	5.3	7.5	1.4	2.6	21:28:01-21:44:41	6.0	23:26:07-23:42:47
$T79*$	2011 DEC 13 (347), 20:11:23	12.9	L-S	4.8	7.2	1.5	5.0	18:12:55-19:02:55	4.6	21:44:50-22:26:30
$T83$	2012 MAY 22 (143), 01:10:11	13.7	L-S	5.2	13.3	2.6	5.6	22:35:38-00:11:41	4.7	02:39:07-04:09:07
$T84$	2012 JUN 07 (159), 00:07:21	13.7	S-S	4.2	6.9	1.6	4.4	23:01:32-23:41:32	4.0	00:28:01-01:28:01
$T86$	2012 SEP 26 (270), 14:35:39	13.5	*	5.6	13.5	2.4	5.6	11:07:56-12:57:30	-	-
$T87$	2012 NOV 13 (318), 10:22:09	13.4	*	2.3	8.9	3.9	-	-	2.3	12:17:34-13:47:34
$T88$	2012 NOV 29 (334), 08:57:00	13.3	S-S	3.6	12.4	3.4	3.9	06:29:30-07:59:30	3.3	11:06:47-12:36:47
$T91$	2013 MAY 23 (143), 17:32:56	12.9	S-S	5.0	15.5	3.1	4.9	14:14:34-15:45:05	5.1	18:16:30-19:46:30
$T92$	2013 JUL 10 (191), 13:21:48	12.8	S-S	4.2	12.4	3.0	4.7	10:18:35-11:48:35	3.8	14:00:49-15:30:49
$T93*$	2013 JUL 26 (207), 11:56:23	12.7	S-S	6.2	12.9	2.1	5.8	10:32:38-11:22:38	6.6	12:45:31-13:35:31
$T94$	2013 SEP 12 (255), 07:43:57	12.6	S-S	4.4	13.4	3.0	3.9	04:53:49-06:23:49	5.0	09:08:26-10:40:33
$T95$	2013 OCT 14 (287), 04:56:28	12.5	S-S	5.5	10.1	1.8	5.3	02:07:44-03:37:44	5.8	06:16:41-07:46:59
$T97$	2014 JAN 01 (001), 21:59:42	12.3	S-S	6.7	13.5	2.0	-	-	6.7	23:20:58-00:50:58
$T98$	2014 FEB 02 (033), 19:12:39	12.3	S-S	5.8	8.1	1.4	5.8	17:02:36-18:32:36	-	-
$T99$	2014 MAR 06 (065), 16:26:48	12.2	S-S	5.8	11.8	2.0	6.1	14:08:05-15:38:08	5.5	17:57:08-19:27:08
$T100$	2014 APR 07 (097), 13:41:15	12.1	L-S	4.4	19.6	4.5	4.4	10:23:14-11:53:14	-	-
$T102$	2014 JUN 18 (169), 13:28:26	23.9	L-L	7.1	9.1	1.3	7.6	11:08:19-12:38:19	6.5	14:12:05-15:42:05
$T103*$	2014 JUL 20 (201), 10:40:58	23.8	L-L	5.5	6.7	1.21	6.5	09:18:10-09:43:10	4.7	11:40:21-12:05:21
$T104*$	2014 AUG 21 (233), 08:09:10	23.8	L-L	5.7	17.5	3.1	5.2	06:11:55-07:26:55	6.5	09:35:16-10:50:16
$T105$	2014 SEP 22 (265), 05:23:20	23.7	L-L	5.7	18.9	3.3	5.8	02:32:35-04:02:35	5.6	07:09:56-08:40:03
$T106$	2014 OCT 24 (297), 02:40:31	23.6	L-L	5.5	23.3	4.2	5.5	23:33:08-01:03:08	5.4	04:25:40-05:55:40
$T108$	2015 JAN 11 (011), 19:48:36	23.4	L-L	5.6	23.5	4.2	6.4	16:54:43-18:24:43	4.9	21:17:26-22:47:26
$T109*$	2015 FEB 12 (043), 17:08:05	23.3	L-L	4.6	12.3	2.7	5.2	15:30:57-16:04:17	4.2	17:45:32-18:02:12
$T110*$	2015 MAR 16 (075), 14:29:49	23.3	L-L	5.2	7.7	1.5	6.4	12:03:11-13:24:06	4.4	15:33:14-16:49:47
$T115$	2016 JAN 16 (016), 02:20:53	2.4	L-L	4.4	6.7	1.5	-	-	4.4	03:59:09-05:29:09
$T116$	2016 FEB 01 (032), 01:01:26	2.4	L-L	6.1	9.2	1.5	-	-	6.1	01:47:54-03:17:54
$T117$	2016 FEB 16 (047), 23:52:04	2.4	L-L	6.0	14.4	2.4	7.2	20:53:57-22:24:40	4.9	01:18:36-02:48:36
$T118$	2016 APR 04 (095), 19:48:00	2.2	L-L	6.8	9.3	1.4	6.7	17:39:57-19:10:00	6.9	21:09:42-22:39:45

REFERENCES

[1] F. M. Neubauer, D. A. Gurnett, J. D. Scudder, and R. E. Hartle, "Titan's magnetospheric interaction," in *Saturn*, T. Gehrels and M. S. Matthews, Eds., University of Arizona Press, Tucson, Arizona, 1984, pp. 760–787.

[2] H. Backes, F. M. Neubauer, M. K. Dougherty, N. Achilleos, N. Andre, C. S. Arridge, C. Bertucci, G. H. Jones, K. K. Khurana, C. T. Russell, and A. Wennmacher, "Titan's magnetic field signature during the first cassini encounter," *Science*, vol. 308, pp. 992–995, 2005.

[3] H. Y. Wei, C. T. Russell, M. K. Dougherty, F. M. Neubauer, and Y. J. Ma, "Upper limits on titan's magnetic moments and implications for its interior," *Journal of Geophysical Research*, vol. 115, E10007, 2010.

[4] F. M. Neubauer, H. Backes, M. K. Dougherty, A. Wennmacher, C. T. Russell, A. Coates, D. Young, N. Achilleos, N. André, C. S. Arridge, C. Bertucci, G. H. Jones, K. K. Khurana, T. Knetter, A. Law, G. R. Lewis, and J. Saur, "Titan's near magnetotail from magnetic field and plasma observations and modelling: Cassini flybys ta, tb, and t3," *J. Geophys. Res.*, vol. 111, A10220, 2006.

[5] C. Bertucci, F. Duru, N. Edberg, M. Fraenz, C. Martinecz, K. Szego, and O. Vaisberg, "The induced magnetospheres of mars, venus, and titan," *Space Sci. Rev.*, vol. 162, pp. 113–171, 2011.

[6] E. Kallio, I. Sillanpaa, and P. Janhunen, "Titan in subsonic and supersonic flow," *Geophysical Research Letters*, vol. 31, p. L15703, 2004.

[7] S. Simon, A. Boßwetter, T. Bagdonat, U. Motschmann, and K.-H. Glassmeier3, "Plasma environment of titan: A 3-d hybrid simulation study," *Ann. Geophys.*, vol. 24, pp. 1113–1135, 2006.

[8] S. Simon and U. Motschmann, "Titan's induced magnetosphere under non-ideal upstream conditions: 3d multi-species hybrid simulations," *Planetary and Space Science*, vol. 57, pp. 2001–2015, 2009.

[9] S. Simon, "Titan's highly variable plasma environment: A 3d hybrid simulation study (Ph.D thesis)," *Technische Universität Braunschweig*, 2007.

[10] S. A. Ledvina, S. H. Brecht, and T. E. Cravens, "The orientation of titan's dayside ionosphere and its effects on titan's plasma interaction," *Earth Planets Space*, vol. 64, pp. 207–230, 2012.

[11] S. Simon, G. Kleindienst, A. Boesswetter, T. Bagdonat, U. Motschmann, K. Glassmeier, J. Schuele, C. Bertucci, and M. K. Dougherty, "Hybrid simulation of titan's magnetic field signature during thecassini t9 flyby," *Geophysical Research Letters*, vol. 34, L24S08, 2007.

[12] N. J. T. Edberg, D. J. Andrews, O. Shebanits, K. Ågren, J. Wahlund, H. J. Opgenoorth, T. E. Cravens, and Z. Girazian, "Solar cycle modulation of titan's ionosphere," *J. Geophys. Res. Space Physics*, vol. 118, pp. 5255–5264, 2013.

[13] S. Simon, E. Roussos, and C. S. Paty, "The interaction between saturn's moons and their plasma environments," *Physcis Reports*, vol. 602, pp. 1–65, 2015.

[14] C. S. Arridge, C. T. Russell, K. K. Khurana, N. Achilleos, S. W. H. Cowley, M. K. Dougherty, D. J. Southwood, and E. J.Bunce, "Saturn's magnetodisc current sheet," *J. Geophys. Res.*, vol. 113, A04214, 2008b.

[15] S. Simon, A. Wennmacher, F. M. Neubauer, C. L. Bertucci, H. Kriegel, J. Saur, C. T. Russell, and M. K. Dougherty, "Titan's highly dynamic magnetic environment: A systematic survey of cassini magnetometer observations from flybys ta–t62," *Planetary and Space Science*, vol. 58, pp. 1230–1251, 2010.

[16] C. S. Arridge, K. K. Khurana, C. T. Russell, D. J. Southwood, N. Achilleos, M. K. Dougherty, A. J. Coates, and H. K. Leinweber, "Warping of saturn's magnetospheric and magnetotail current sheets," *J. Geophys. Res.*, vol. 113, A08217, 2008a.

[17] S. Kabanovic, S. Simon, F. M. Neubauer, and Z. Meeks, "An empirical model of titan's magnetic environment during the cassini era: Evidence for seasonal variability," *J. Geophys. Res.*, vol. 122, pp. 11 076–11 085, 2017.

[18] C. Bertucci, B.Sinclair, N.Achilleos, P.Hunt, M.K.Dougherty, and C.S.Arridge, "The variability of titan's magnetic environment," *Planetary and Space Science*, vol. 57, pp. 1813–1820, 2009.

[19] E. Sittler, R. Hartle, R. Johnson, J. Copper, A. Lipatov, C. Bertucci, A. Coates, K. Szego, M. Shappirio, D. Simpson, and J.-E Wahlund, "Saturn's magnetospheric interaction with titan as defined by cassini encounters t9 and t18: New results," *Planetary and Space Science*, vol. 58 (3), pp. 327–350, 2010.

[20] K. Szego, Z. Nemeth, G. Erdos, L. Foldy, M. Thomsen, and D. Delapp, "The plasma environment of titan: The magnetodisk of saturn near the encounters as derived from ion densities measured by the cassini/caps plasma spectrometer," *J. Geophys. Res.*, vol. 116, A10219, 2011.

[21] D. J. Andrews, S. W. H. Cowley, M. K. Dougherty, and G. Provan, "Magnetic field oscillations near the planetary period in saturn's equatorial magnetosphere: Varia-

tion of amplitude and phase with radial distance and local time," *J. Geophys. Res.*, vol. 115, A4, 2010.

[22] S. Simon, S. C. van Treeck, A. Wennmacher, J. Saur, F. M. Neubauer, C. L. Bertucci, and M. K. Dougherty, "Structure of titan's induced magnetosphere under varying background magnetic field conditions: Survey of cassini magnetometer data from flybys ta–t85," *J. Geophys. Res.*, vol. 118, pp. 1679–1699, 2013.

[23] S. Simon, A. Boesswetter, T. Bagdonat, U. Motschmann, and J. Schuele, "Three-dimensional multispecies hybrid simulation of titan's highly variable plasma environment," *Ann. Geophys.*, vol. 25, pp. 117–144, 2007.

[24] J.-E. Wahlund, R. Bostrom, G. Gustafsson, D. Gurnett, W. Kurth, A. Pedersen, T. Averkamp, G. Hospodarsky, A. Persoon, P. Canu, F. Neubauer, M. Dougherty, A. Eriksson, M. Morooka, R. Gill, M. Andre, L. Eliasson, and I. Muller-Wodarg, "Cassini measurements of cold plasma in the ionosphere of titan," *Science*, vol. 308, pp. 7986–989, 2005.

[25] S. Simon, U. Motschmann, G. Kleindienst, J. Saur, C. L. Bertucci, M. K. Dougherty, C. S. Arridge, and A. J. Coates, "Titan's plasma environment during a magnetosheath excursion: Real-time scenarios for cassini's t32 flyby from a gybrid simulation," *Ann. Geophys.*, vol. 27, pp. 669–685, 2009.

[26] H. Y. Wei, C. T. Russell, M. K. Dougherty, Y. J. Ma, K. C. Hansen, H. J. McAndrews, A. Wellbrock, A. J. Coates, M. F. Thomsen, and D. T. Young, "Unusually strong magnetic fields in titan's ionosphere: T42 case study," *Advances in Space Research*, vol. 48, pp. 314–322, 2011.

[27] N. J. T. Edberg, D. J. Andrews, O. Shebanits, K. Agren, J. E Wahlund, H. J. Opgenoorth, E. Roussos, P. Garnier, T. E. Cravens, S. V. Badman, R. Modolo, C. Bertucci, and M. K. Dougherty, "Extreme densities in titan's ionosphere during the t85 magnetosheath encounter," *Geophysical Research Letters*, vol. 40, pp. 2879–2883, 2013.

[28] H. McAndrews, M. Thomsen, C. Arridge, C. Jackman, R. Wilson, M. Henderson, R. Tokar, K. Khurana, E. Sittler, A. Coates, and M. Dougherty, "Plasma in saturn's nightside magnetosphere and the implications for global circulation," *Planetary and Space Science*, vol. 57, no. 14, pp. 1714 –1722, 2009.

[29] A. M. Rymer, H. T. Smith, A. Wellbrock, A. J. Coates, and D. T. Young, "Discrete classification and electron energy spectra of titan's varied magnetospheric environment," *Geophysical Research Letters*, vol. 36, no. 15, p. L15109, 2009.

[30] H. T. Smith and A. M. Rymer, "An empirical model for the plasma environment along titan's orbit based on cassini plasma observations," *Journal of Geophysical Research: Space Physics*, vol. 119, no. 7, pp. 5674–5684, 2014.

[31] C. S. Arridge, N. Achilleos, and P. Guio, "Electric field variability and classifications of titan's magnetoplasma environment," *Annales Geophysicae*, vol. 29, no. 7, pp. 1253–1258, 2011.

[32] C. Bertucci, N. Achilleos, M. K. Dougherty, R. Modolo, A. J. Coates, K. Szego, A. Masters, Y. Ma, F. M. Neubauer, P. Garnier, J.-E. Wahlund, and D. T. Young, "The magnetic memory of titan's ionized atmosphere," *Science*, vol. 321, pp. 1475–1478, 2008.